ChemComm

Controllable Transformation Between 3D and 2D Perovskites through Cation Exchange

Journal:	*ChemComm*
Manuscript ID	CC-COM-05-2018-004261.R1
Article Type:	Communication

Chemical Communications

COMMUNICATION

Controllable Transformation Between 3D and 2D Perovskites through Cation Exchange

Received 00th January 20xx,
Accepted 00th January 20xx

DOI: 10.1039/x0xx00000x

www.rsc.org/

Weixin Huang, [a,#] Yuanxing Wang[b,#] and Subila K. Balakrishnan*[a]

A facile post-synthetic cation exchange approach has been employed to controllably tune the optical and structural properties of colloidal perovskite nanocrystals (NCs). These optical changes are attributed to the structural transformation of perovskite NCs from the three-dimensional (3D) to the two-dimensional (2D) layered crystalline forms and vice versa.

Hybrid organic-inorganic perovskites have recently emerged as one of the most promising semiconductor materials for low-cost optoelectronic and photonic devices, due to their outstanding optical and electrical properties.[1,2] While the main focus of perovskite materials has been on photovoltaic technology, these materials also show considerable potential in applications such as LEDs and lasers.[3,4] Green-emitting three-dimensional (3D) methylammonium lead bromide ($MAPbBr_3$) perovskites exhibit high photoluminescence (PL) quantum efficiencies up to 90 %.[5] Besides the high PL quantum efficiencies, the perovskite materials also show wide wavelength tunability throughout the visible range owing to their synthetically fine-tuned crystalline architectures.

The two-dimensional (2D) layered perovskites show excellent optical properties with blue-shifted emission because of the quantum confinement effect from the dimensional reduction of hybrid perovskites.[6,7] It is reported that, by increasing the ligand concentration, the synthesized 2D hybrid perovskites show the tunable PL emission.[8] Recently, the post-synthetic transformation of lead-halide perovskites provides an opportunity to flexibly and reversibly tune their optical and electronic properties.[9–11] This kind of flexibility in tuning the band gap of the same materials under ambient conditions is desirable for the optoelectronic applications.[12–14] However, there remains an omission in the study of the reversibly tuning of band gap in colloidal hybrid perovskite NCs via post-synthetic reactions with cations. Herein, we propose a facile approach to controllably tune the PL emission and structure of hybrid perovskite NCs via post-synthesis cation exchange reaction. Our findings provide an alternative approach for the preparation of bandgap-tunable perovskite crystals, developing a better understanding of versatile hybrid perovskites and their design through chemical post-synthetic transformations.

We synthesized 3D $MAPbBr_3$ NCs following the method reported previously[15]. It is interesting that, with the introduction of PEA^+, the 3D $MAPbBr_3$ NCs solutions under ultraviolet (UV) illumination show a change in the emission color, green to violet (Figure 1A, Step 1). Figure 1B shows the absorption and emission spectra of the as-synthesized 3D $MAPbBr_3$ NCs (0.72 µmol in 5 ml) before and after addition of 2.8 µmol PEA^+. In the as-synthesized solution, the PL peak appears at 518 nm and the UV-Visible absorption spectrum shows a band edge at 506 nm, consistent with the previously reported value for 3D $MAPbBr_3$ NCs.[16] By adding PEA^+ to the solution, the PL emission peak shifts to 411 nm, with analogous blue shifts in the absorption spectra (Figure 1B).

The blue shifts observed in PL and the absorption spectra are reminiscent of the quantum confinement effect reported previously in the lamellar architectures of 2D perovskites.[6] To understand the effect of PEA^+ on the optical change of 3D $MAPbBr_3$ NCs, we performed X-ray diffraction (XRD) measurements. As displayed in Figure 1C, the peaks at 2θ values of 14.5° and 29.5° for the $MAPbBr_3$ sample correspond to the diffractions from (110) and (220) planes, respectively, indicating the formation of 3D tetragonal perovskite structure.[16] Nonetheless, new peaks at smaller angles (5°, 10.5°, 15.7°, 21.1°, 26.5° and 32.0°) appear in the post-synthetic sample, which indicate the formation of 2D perovskite nanostructure with n = 1 monolayer.[7] The appearance of tiny peaks at 4.0° and 8.2° might be due to the reaction between $(PbX_6)^{4-}$ and residual ligand-octylamine, forming 2D $(OcA)_2PbBr_4$ perovskite.

The above results show that the transformation of 3D to 2D perovskite by the post-synthetic introduction of new cations, it is worthwhile to identify the possibility of the reaction reversibility (2D to 3D transformation). To investigate this possibility, the 2D $(OcA)_2PbBr_4$ perovskite NCs were first synthesized according to a previously reported procedure.[7]

[a] Radiation Laboratory, Department of Chemistry and Biochemistry, University of Notre Dame, Notre Dame, IN 46556, USA. E-mail: subilakb@gmail.com
[b] Institute of Advanced Synthesis, School of Chemistry and Molecular Engineering, Jiangsu National Synergetic Innovation Center for Advanced Materials, Nanjing Tech University, Nanjing, 211816, P. R. China.
[#] These authors contributed equally to this work.
†Electronic Supplementary Information (ESI) available. See DOI: 10.1039/x0xx00000x

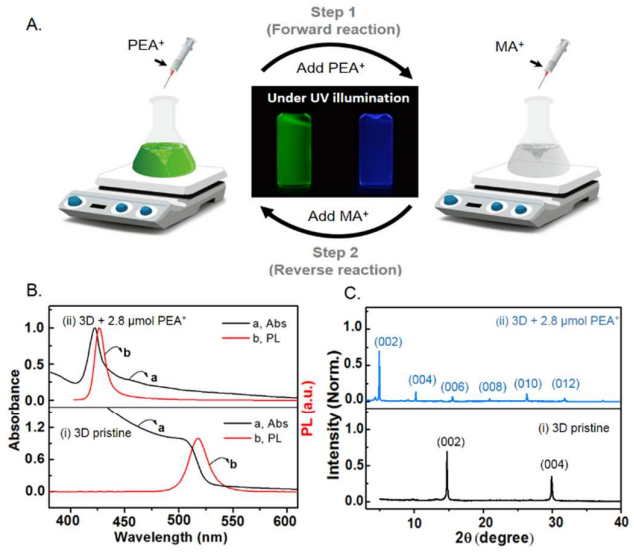

Figure 1. (A) Schematic illustration of the controllable transformation of 3D-2D perovskites through cation exchange. (B) UV-visible absorption (black line, a) and PL emission (red line, b) spectra of (i) the as-synthesized 3D $MAPbBr_3$ sample (0.72 µmol in 5 ml) and (ii) the as-synthesized 3D sample with the addition of 2.8 µmol of PEA^+. And (C) XRD patterns of (i) the as-synthesized 3D $MAPbBr_3$ sample (0.72 µmol in 5 ml) and (ii) the as-synthesized sample with the addition of 2.8 µmol of PEA^+.

Figure 2A illustrates the PL and absorption spectra of the as-synthesized 2D perovskite NCs (0.72 µmol in 5 ml), exhibiting an absorption peak at 398 nm and an emission peaks at 408 nm, which are in agreement with the reported literature.[6] With the addition of 1.0 µmol of MA^+, the PL emission of perovskite NCs red-shifts to 525 nm. Consistent with the PL emission change, the absorption band edge of the perovskite NCs also shifts to the value of 519 nm. Figure 2B shows the XRD patterns obtained from the perovskite NCs before and after the addition of MA^+. For the as-synthesized 2D perovskite sample, XRD peaks at 4.0°, 8.2° and 12.3° are characteristic of 2D perovskite structure with n = 1 monolayer.[7] After adding MA^+, the post-synthetic sample exhibits the diffraction peaks observed at 14.5° and 29.5°, which arise due to the formation of 3D $MAPbBr_3$ perovskite NCs.[16]

Figures S1A and B show transmission electron microscopy (TEM) images of the as-synthesized 3D $MAPbBr_3$ sample and the post-synthetic sample with the addition of PEA^+. In the as-synthesized sample, the lateral size of 3D $MAPbBr_3$ NCs is estimated to be of 6.3 ± 2 nm (Figure S1A), consistent with the reported literature.[15] A similarity was observed in the size of NCs (4.6 ± 1 nm) after adding PEA^+. The TEM images of perovskite NCs from the reverse reaction (Figure S1C and D) show the similar change in sizes as those from the forward reaction. To evaluate the height of the NCs, we have performed atomic force microscopy (AFM) (Figure S2). As shown in Figure S2A, the as-synthesized 3D $MAPbBr_3$ NCs exhibit the NCs thickness of ~11.3 nm. The AFM analysis on the post-synthetic 2D sample with the addition of PEA^+ showed a thickness of ~4.2

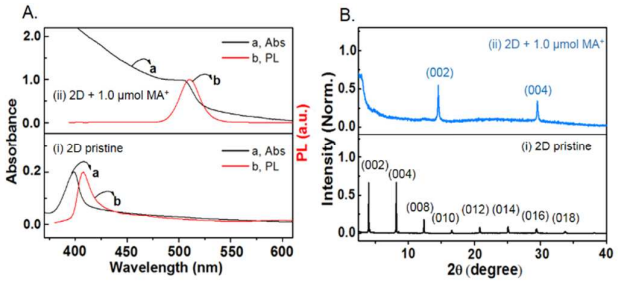

Figure 2. (A) UV-visible absorption (black line, a) and PL emission (red line, b) spectra of (i) the as-synthesized 2D $(OcA)_2PbBr_4$ sample (0.72 µmol in 5 ml) and (ii) the as-synthesized 2D sample with the addition of 1.0 µmol of MA^+. (B) XRD patterns of (i) the as-synthesized 2D $(OcA)_2PbBr_4$ sample (0.72 µmol in 5 ml) and (ii) the as-synthesized sample with the addition of 1.0 µmol of MA^+.

nm (Figure S2B). The decrease in thickness indicates that the 2D layered perovskite NCs experience the exfoliation process,[17] in which the intercalation of long-chain alkylammonium species causes the formation of weakly bonded layers, followed by the delamination of the layered structures into individual layers.

The excited state lifetime measurements for the samples after the forward as well as reverse cation exchange reactions in solutions were carried out using Time Correlated Single Photon Counting (TCSPC) analysis (Figure 3A). The lifetime values are listed in the Table S1. The as-synthesized samples show an average lifetime of 17.83 ns and decreases to 5.57 ns with the addition of PEA^+. In addition, a decrease in the PL quantum yield was observed from 62 to 33 % after introducing PEA^+ (Figure S3). The drastical decrease in PLQY was also observed in our recent publication while 3D $CsPbBr_3$ perovskites were converted into their 2D counterparts.[11] The PLQY decrease may be due to the introduction of defect states during structural transformation. In addition, the emission in perovskite originates from the recombination of free charge carriers due to low exciton binding energy.[13] Therefore, a decrease in the PL decay lifetime indirectly confirms the transformation of 3D to 2D perovskites. In the reverse reaction, the PL decay lifetime of NCs increased from 0.37 to 12.43 ns (Figure 3A) and PL quantum yield increased from 5 to 72 % (Figure S3). The increase in an average lifetime and PL quantum yield with the addition of MA^+ indicates the transformation of 2D to 3D perovskite structure as seen in our spectroscopic and microscopic analysis.

In addition, this post-synthetic process is highly versatile as the forward reaction not only works for PEA^+ but also for other long chain ammonium cations-octylammonium (OcA^+) and butylammonium (BA^+) ions, which are also used as ligands to control the crystallization of perovskite NCs.[6] With the addition of OcA^+ or BA^+, the same trend in the change of PL emission spectra of the as-synthesized perovskite NCs were observed (Figure S4A and C). The appearance of new XRD peaks in the lower angles prove the formation of 2D perovskite NCs (Figure S4B and D).[7,18] To verify the versatility of the reverse reaction, we replaced MA^+ from the reaction with another small ammonium cation-cesium ion, Cs^+. Similar to the addition of MA^+, the perovskite NCs displayed a red shift in the PL and the absorption spectra with the addition of Cs^+ (Figure S5A). The

formation of the 3D perovskite NCs is confirmed by the XRD pattern (Figure S5B).[11]

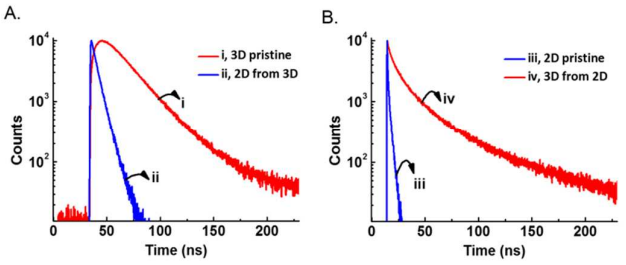

Figure 3. (A and B) Time resolved PL decay traces the as-synthesized 3D $MAPbBr_3$ NCs (0.72 µmol in 5 ml) (i- red trace), the as-synthesized perovskite sample (0.72 µmol in 5 ml) with the addition of 2.8 µmol PEA^+ (ii- blue trace), the as-synthesized 2D $(OcA)_2PbBr_4$ NCs (0.72 µmol in 5 ml) (iii- blue trace), and the as-synthesized 2D $(OcA)_2PbBr_4$ NCs (0.72 µmol in 5 ml) with the addition of 1.0 µmol MA^+ (iv- red trace).

To validate the hypothesis of the transformation being induced by cation exchange, we studied the forward and reverse reactions by using ambient pressure X-ray photoelectron spectroscopy (AP-XPS). In the forward reaction, the chemical evolution of the as-synthesized 3D $MAPbBr_3$ perovskite films under exposure to butylamine (BA) was examined. BA is chosen for the forward reaction since it has higher vapor pressure (90 mbar) than that of PEA (0.3 mbar) at room temperature.[19] Figures 4A and S6 show the C 1s, N 1s, Pb 4f, and Br 3d photoelectron spectra of $MAPbBr_3$ perovskite prior to and after exposing to BA vapor (0.5 mbar) from 7 hours. Under BA treatment, the successful conversion of 3D perovskite into 2D perovskite was achieved, as shown by the XRD measurement (Figure S7).[18] In Figure 4A, the XPS spectrum measured from the pristine film shows two peaks at 285.3 and 286.6 eV in C 1s spectra, which are attributed to adventitious carbon and carbon from the methylammonium cation, respectively.[20–23] Upon exposure to BA, there is an increase in C1s peak at 285.3 eV (Figure 4A, spectrum ii). The enhanced peak intensity originates from the formation of BA cations in the film since the hydrocarbon ($-CH_2-$) has the same binding energy at 285.3 eV.[10,22,24] Quantitative analysis in Figure 4B shows that the $C/C_{pristine}$ increases from approximately 1 to 1.5 after the treatment of BA, further indicating the existence of BA^+ ions. The reverse reaction was studied by exposing the 2D perovskite sample (BA-treated perovskite film) to methylamine (MA) gas (0.5 mbar) for 7 hours. The XRD pattern of the resulting film displays a new diffraction peak at 14.5°, representing the formation of 3D $MAPbBr_3$ perovskite (Figure S7). Figure 4A and B show that with the exposure to MA, the XPS spectrum of the perovskite film exhibits a decrease in the C1s peak at 285.3 eV and $C/C_{pristine}$ ratio drops from 1.5 to 1.1. Both of these results suggest the loss of BA^+ in the perovskite film. In contrast to the varying $C/C_{pristine}$ ratios, no distinguishable changes were observed in $N/N_{pristine}$ ratios after the forward and reverse reactions (Figure S8), which implies that the nitrogen-containing species remain unchanged within the perovskite structure. The constant $N/N_{pristine}$ and changing $C/C_{pristine}$ ratios suggest that the reversible 3D-2D perovskite transformation is achieved through equimolar substitution of BA^+ and MA^+, in which the reversible substitution between these two cations occurs through a proton

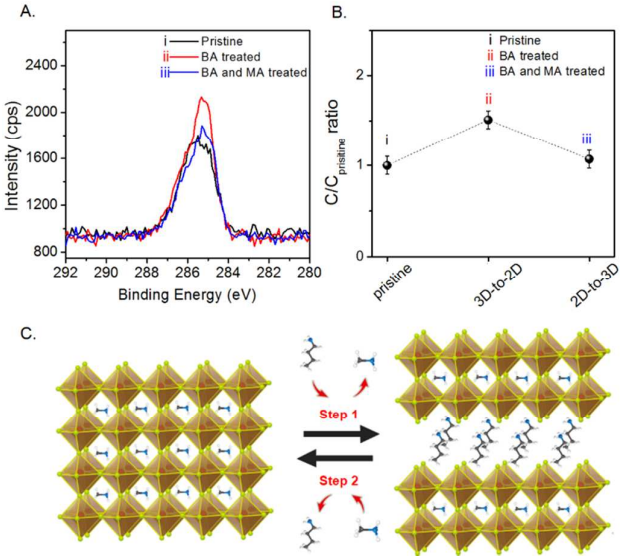

Figure 4. (A) C 1s photoelectron spectra of (i) the pristine $MAPbBr_3$ film, (ii) the $MAPbBr_3$ film obtained after the exposure of BA, and (iii) the $MAPbBr_3$ film obtained after consecutive exposure to BA and MA, and (B) the change of carbon content in these three films. And (C) Schematic of the reversible transformation of 3D-2D perovskites in the solution (the proposed chemical equations are given in the supporting information).

transfer mechanism (Figure S9).[10] Therefore, the *in-situ* AP-XPS studies support the experimental observations of the optical and structural evolution of colloidal perovskite NCs.

The above experimental findings reveal that the reversible 3D–2D transformation of perovskites can triggered by the post-synthetical introduction of foreign cations. A plausible reaction mechanism was proposed to explain this transformation (Figure 4C and reaction S1 and S2). The structure of 3D hybrid $MAPbBr_3$ perovskite consists of the alternate stacking of organic/inorganic layers, in which the organic layer (cation) interacts with the inorganic layer ($(PbX_6)^{4-}$ part) through ionic interactions. Upon the addition of a foreign cation (e.g. BA^+), the cation exchange reaction occurs and it leads to the formation of the 2D layered perovskites (Step 1 in Figure 4C). In the reverse reaction, the substitution between BA^+ and MA^+ took place while MA^+ was introduced to the solution (Step 2 in Figure 4C).

In conclude, we reported a facile post-synthesis cation exchange approach to controllably tune the structure of $MAPbBr_3$ NCs. By adding long chain cations (PEA^+) and small cations (MA^+), the structure transformation of NCs between 3D and 2D can be realized during the forward and reverse reactions. The obtained 3D and 2D perovskite NCs exhibit the changes in PL emission, sample thickness and PL decay lifetime. The ease of the synthesis via cation exchange, as well as its great versatility in tuning the bandgap and photo physical properties, make this method applicable in processing perovskite NCs for solar cell as well as LED devices.

The authors thank Dr. Sylwia Ptasinska and Dr. Prashant V. Kamat for their helpful guidance and input. W.H. and S.K.B acknowledge the support of the Division of Chemical Sciences, Geosciences, and Biosciences, Office of Basic Energy Sciences of the U.S. Department of Energy, through Award DE-FC02-04ER15533. This is contribution number NDRL 5181 from the Notre Dame Radiation Laboratory. Y.W. thanks China Postdoctoral Administration and Nanjing Tech University for a postdoctoral fellowship. The authors thank the cSEND Materials Characterization Facility for the use of the Bruker pXRD.

Conflicts of interest

There are no conflicts to declare

Notes and references

1 H. Zhou, Q. Chen, G. Li, S. Luo, T. -b. Song, H.-S. Duan, Z. Hong, J. You, Y. Liu and Y. Yang, Science, 2014, 345, 542–546.
2 J. S. Manser, J. A. Christians and P. V. Kamat, Chem. Rev., 2016, 116, 12956–13008.
3 H. Cho, S.-H. Jeong, M.-H. Park, Y.-H. Kim, C. Wolf, C.-L. Lee, J. H. Heo, A. Sadhanala, N. Myoung, S. Yoo, S. H. Im, R. H. Friend and T.-W. Lee, Science, 2015, 350, 1222–1225.
4 Z. Xiao, R. A. Kerner, L. Zhao, N. L. Tran, K. M. Lee, T.-W. Koh, G. D. Scholes and B. P. Rand, Nat. Photonics, 2017, 11, 108–115.
5 H. Huang, A. S. Susha, S. V. Kershaw, T. F. Hung and A. L. Rogach, Adv. Sci., 2015, 2, 1500194.
6 Z. Yuan, Y. Shu, Y. Xin and B. Ma, Chem. Commun., 2016, 52, 3887–3890.
7 S. Gonzalez-Carrero, G. M. Espallargas, R. E. Galian and J. Pérez-Prieto, J. Mater. Chem. A, 2015, 3, 14039–14045.
8 J. A. Sichert, Y. Tong, N. Mutz, M. Vollmer, S. Fischer, K. Z. Milowska, R. García Cortadella, B. Nickel, C. Cardenas-Daw, J. K. Stolarczyk, A. S. Urban and J. Feldmann, Nano Lett., 2015, 15, 6521–6527.
9 G. Li, T. Zhang, N. Guo, F. Xu, X. Qian and Y. Zhao, Angew. Chemie Int. Ed., 2016, 55, 13460–13464.
10 W. Huang, J. S. Manser, S. Sadhu, P. V. Kamat and S. Ptasinska, J. Phys. Chem. Lett., 2016, 7, 5068–5073.
11 S. K. Balakrishnan and P. V. Kamat, Chem. Mater., 2018, 30, 74–78.
12 Z. Guo, X. Wu, T. Zhu, X. Zhu and L. Huang, ACS Nano, 2016, 10, 9992–9998.
13 Y. Tong, F. Ehrat, W. Vanderlinden, C. Cardenas-Daw, J. K. Stolarczyk, L. Polavarapu and A. S. Urban, ACS Nano, 2016, 10, 10936–10944.
14 P. Chen, Y. Bai, S. Wang, M. Lyu, J.-H. Yun and L. Wang, Adv. Funct. Mater., 2018, 28, 1706923.
15 H. Huang, F. Zhao, L. Liu, F. Zhang, X. Wu, L. Shi, B. Zou, Q. Pei and H. Zhong, ACS Appl. Mater. Interfaces, 2015, 7, 28128–28133.
16 L. Liu, S. Huang, L. Pan, L.-J. Shi, B. Zou, L. Deng and H. Zhong, Angew. Chemie Int. Ed., 2017, 56, 1780–1783.
17 A. A. Jeffery, A. Pradeep and M. Rajamathi, Phys. Chem. Chem. Phys., 2016, 18, 12604–12609.
18 D. H. Cao, C. C. Stoumpos, O. K. Farha, J. T. Hupp and M. G. Kanatzidis, J. Am. Chem. Soc., 2015, 137, 7843–7850.
19 I. Mokbel, A. Razzouk, T. Sawaya and J. Jose, J. Chem. Eng. Data, 2009, 54, 819–822.
20 S. Chen, T. W. Goh, D. Sabba, J. Chua, N. Mathews, C. H. A. Huan and T. C. Sum, APL Mater., 2014, 2, 081512/1–081512/7.
21 W. Huang, J. S. Manser, P. V. Kamat and S. Ptasinska, Chem. Mater., 2016, 28, 303–311.
22 A. R. Milosavljević, W. Huang, S. Sadhu and S. Ptasinska, Angew. Chemie, 2016, 55, 10083–10087.
23 W. Huang, S. Sadhu and S. Ptasinska, Chem. Mater., 2017, 29, 8478–8485.
24 S. Alexander, L. Morrow, A. M. Lord, C. W. Dunnill, A. R. Barron and A. R. Barron, J. Mater. Chem. A, 2015, 3, 10052–10059.

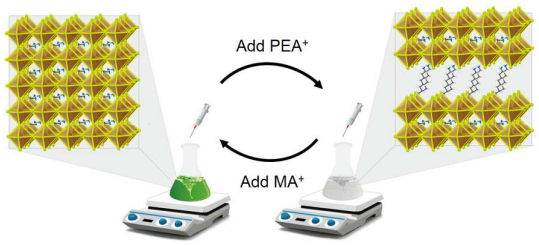

Transformation between 3D and 2D perovskites can be controlled through post-synthetic introduction of foreign cations.